



# Recent Developments in Speeding up Prostate MRI

Nida Mir, MSc,<sup>1\*</sup>  Stefan J. Fransen, MSc,<sup>2</sup>  Jelmer M. Wolterink, PhD,<sup>3</sup>  
Jurgen J. Fütterer, MD, PhD,<sup>4,5</sup> and Frank F.J. Simonis, PhD<sup>1</sup>

The increasing incidence of prostate cancer cases worldwide has led to a tremendous demand for multiparametric MRI (mpMRI). In order to relieve the pressure on healthcare, reducing mpMRI scan time is necessary. This review focuses on recent techniques proposed for faster mpMRI acquisition, specifically shortening T2W and DWI sequences while adhering to the PI-RADS (Prostate Imaging Reporting and Data System) guidelines. Speeding up techniques in the reviewed studies rely on more efficient sampling of data, ranging from the acquisition of fewer averages or *b*-values to adjustment of the pulse sequence. Novel acquisition methods based on undersampling techniques are often followed by suitable reconstruction methods typically incorporating synthetic priori information. These reconstruction methods often use artificial intelligence for various tasks such as denoising, artifact correction, improvement of image quality, and in the case of DWI, for the generation of synthetic high *b*-value images or apparent diffusion coefficient maps. Reduction of mpMRI scan time is possible, but it is crucial to maintain diagnostic quality, confirmed through radiological evaluation, to integrate the proposed methods into the standard mpMRI protocol. Additionally, before clinical integration, prospective studies are recommended to validate undersampling techniques to avoid potentially inaccurate results demonstrated by retrospective analysis. This review provides an overview of recently proposed techniques, discussing their implementation, advantages, disadvantages, and diagnostic performance according to PI-RADS guidelines compared to conventional methods.

**Level of Evidence:** 3

**Technical Efficacy:** Stage 3

J. MAGN. RESON. IMAGING 2023.

Globally, prostate cancer (PCa) is the second most common form of cancer in men. With more than 1.4 million new cases of PCa reported in 2020, it remained the fifth leading cause of cancer-related death among men.<sup>1</sup> This number is expected to grow to 2.4 million cases by 2040.<sup>2</sup> Over the past two decades, 65 countries have experienced an increase in age-standardized PCa incidence rates, while 19 countries have seen an increase in age-standardized mortality rates.<sup>1</sup> Clinically significant prostate tumors need to be detected well in time to initiate curative treatment.

Multiparametric magnetic resonance imaging (mpMRI) is used to detect, localize, and stage prostate tumors.<sup>3</sup> mpMRI has emerged as a valuable tool for improving the accuracy of

prostate cancer diagnosis and risk stratification, leading to a gradual yet noteworthy increase in the utilization of mpMRI in active surveillance.<sup>4</sup> Technical guidelines for mpMRI acquisition for PCa called the prostate imaging reporting and data system (PI-RADS v2.1) are published by the European Society of Urogenital Radiology (ESUR).<sup>5</sup> These guidelines ensure standardization and consistency in the implementation of mpMRI across hospitals. The PI-RADS protocol includes T1-weighted imaging (T1WI), T2-weighted imaging (T2WI), and diffusion-weighted imaging (DWI), supplemented by dynamic contrast-enhanced (DCE) MRI. The introduction of PI-RADS has led to uniform reporting of prostate lesions and wider acceptance of mpMRI for the

View this article online at [wileyonlinelibrary.com](http://wileyonlinelibrary.com). DOI: 10.1002/jmri.29108

Received Jul 24, 2023, Accepted for publication Oct 17, 2023.

\*Address reprint requests to: N.M., Magnetic Detection and Imaging, Technical Medical Centre 2186. University of Twente, Drienerlolaan 5, 7522 NB, Enschede, Netherlands. E-mail: [n.mir@utwente.nl](mailto:n.mir@utwente.nl)

From the <sup>1</sup>Magnetic Detection and Imaging, Technical Medical Centre, University of Twente, Enschede, Netherlands; <sup>2</sup>Department of Radiology, University Medical Center Groningen, Groningen, Netherlands; <sup>3</sup>Department of Applied Mathematics, Technical Medical Centre, University of Twente, Enschede, Netherlands; <sup>4</sup>Robotics and Mechatronics, Technical Medical Centre, University of Twente, Enschede, Netherlands; and <sup>5</sup>Minimally Invasive Image-Guided Interventions Center, Department of Medical Imaging, Radboud University Medical Center, Nijmegen, Netherlands

This is an open access article under the terms of the [Creative Commons Attribution](https://creativecommons.org/licenses/by/4.0/) License, which permits use, distribution and reproduction in any medium, provided the original work is properly cited.

detection and active surveillance of PCa.<sup>4,6</sup> As the demand for mpMRI scans continues to increase, the healthcare system is experiencing mounting pressure. A faster acquisition scheme for mpMRI could reduce strain on current resources. Such a scheme should speed up acquisition but also retain the specificity and sensitivity of mpMRI.

This review highlights novel approaches aimed at reducing the scan time of the mpMRI protocol. The PI-RADS protocol summarized in Table 1 lays out guidelines for mpMRI acquisition for the detection of PCa. Of the four sequences included in PI-RADS, shortening T2WI and DWI sequences is considered to have the most impact on protocol length. First, T2WI and DWI contribute to a major portion of the total scan time, while the acquisition of T1WI is relatively fast. Second, the imaging time for contrast-based DCE MRI depends on the wash-in rate of the contrast and physiological processes, and hence, the acquisition time of DCE MRI cannot be controlled externally. For these reasons, this review is focused on techniques proposed for speeding up T2WI and DWI. Moreover, this review highlights techniques speeding up mpMRI by shortening the acquisition time and not by the omission of standard recommended sequences. The reviews of Hotker et al.<sup>7</sup> and Girometti et al.<sup>8</sup> discuss the performance, scan time, and throughput of the bi-parametric MRI (bpMRI) protocol, that is, omission of DCE MRI, and the effect of

DCE and eliminating it in detail. Hence, we consider studies that report speeding up by exclusion of PI-RADS recommended scans beyond the scope of the review. This includes 1) using the “bi-parametric MRI (bpMRI)” protocol, 2) using the “fast bpMRI,” that is, acquiring T2WI in a single plane, rather than the recommended minimum of two planes in addition to the omission of DCE MRI, or 3) using mono-parametric MRI, that is, solely acquiring the apparent diffusion coefficient (ADC) ratios based on advanced DWI.

## Materials and Methods

### Literature Search

The preferred reporting items for systematic reviews and meta-analysis extension for scoping reviews (PRISMA) model was used to select studies based on the inclusion criteria for this study.<sup>9</sup> The databases of Scopus, PubMed, and Web of Science were searched on January 3, 2023, using the terms “MRI” and “prostate” in addition to synonyms of the terms “short,” “fast,” “acquisition,” “imaging,” and “technique.”

### Study Selection Criteria

This narrative review describes developments proposed for speeding up mpMRI by altering the imaging sequence and subsequent reconstruction. Included articles were published from the year 2018 onwards, written in English, conducted on humans, and reported techniques proposed for speeding up the PI-RADS recommended mpMRI protocol. The list of documents produced was reviewed, and studies were excluded if they 1) did not report on speeding up of PCa MRI acquisition, 2) reported speeding up by using bpMRI or Abbreviated bpMRI protocol, or 3) reported on techniques not recommended in the PI-RADS mpMRI protocol.

### Data Collection and Extraction

A full-text review of the selected studies was performed to retrieve the proposed technique for speeding up mpMRI acquisition, how the technique was implemented, the expected impact of the technique on the mpMRI acquisition time, and performance based on qualitative metrics (e.g., lesion conspicuity, artifacts, background noise suppression, sharpness of anatomic structures, overall image quality and diagnostic confidence) and quantitative metrics (e.g., signal-to-noise ratio (SNR), peak signal-to-noise ratio (PSNR) contrast-to-noise ratio (CNR), structural similarity index measure (SSIM), root mean squared error (RMSE), feature similarity index measure (FSIM), etc.).

## Results

Figure 1 shows the results of our search queries and the selection of studies included in this review. Out of 5325 studies identified from Scopus, Web of Science, and Pubmed databases, 31 studies were included in this review based on the inclusion criteria stated in the methods section.

The results of this review have been divided into two sections: speeding up T2WI and speeding up DWI. The subsections describe different techniques suitable for each sequence. A description of the technical implementation and the impact of the technique on the overall protocol is given.

**TABLE 1. PI-RADS Protocol for PCa MRI**

Sequence	Guidelines
T1WI	Axial plane
T2WI	Axial plane and a minimum of one additional orthogonal plane (i.e., sagittal and/or coronal)
DWI	One low <i>b</i> -value preferably ( <i>b</i> -50 – <i>b</i> -100) and one intermediate <i>b</i> -value set ( <i>b</i> -800 – <i>b</i> -1000) for ADC maps.
	High <i>b</i> -value set ( $\geq b$ -1400) obtained from a separate acquisition or calculated from the low and intermediate <i>b</i> -value images.
	Imaging planes are the same as those used for T2WI.
DCE MRI	Carried out for several minutes to assess the enhancement characteristics.
	Imaging planes are the same as those used for T2WI and DWI.

T1WI = T1-weighted imaging; T2WI = T2-weighted imaging; DWI = diffusion weighted imaging; DCE = dynamic contrast-enhanced.

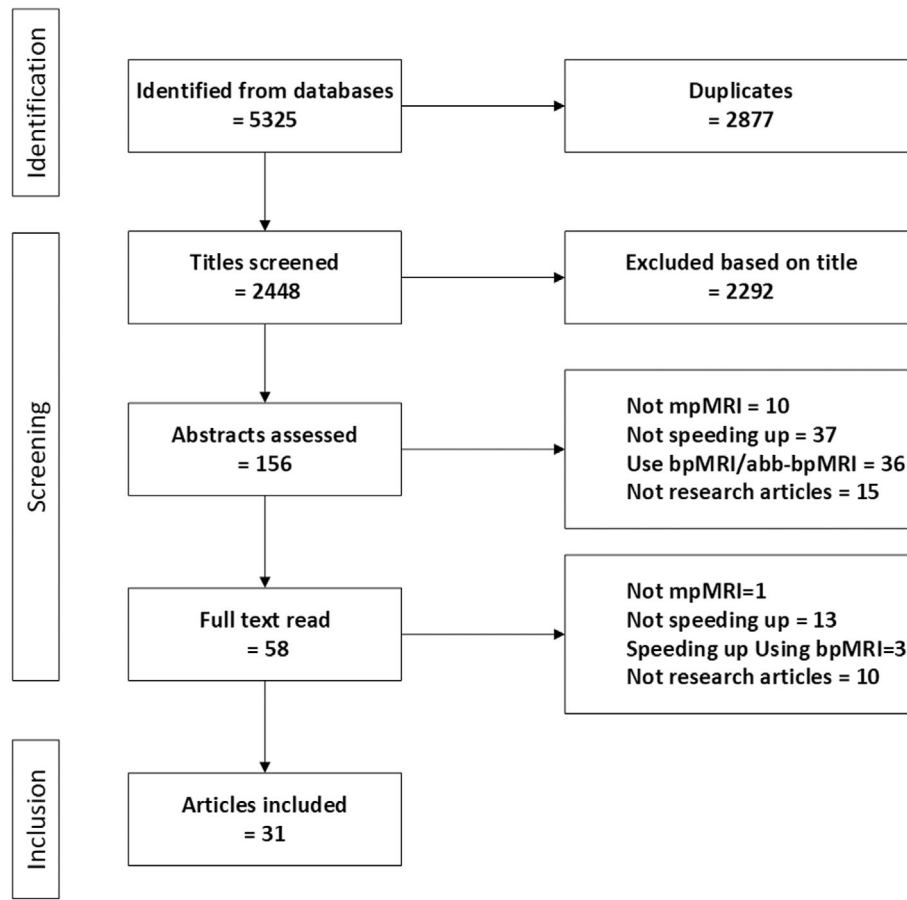


FIGURE 1: PRISMA flowchart of the study selection process.

### Speeding up T2-Weighted Imaging

T2W scans are important for lesion detection in the prostate and for differentiating its zonal anatomy and account for ~60% of the protocol acquisition time. The PI-RADS guidelines recommend acquiring T2W scans in the axial plane and a minimum of one additional orthogonal plane with a slice thickness of 3 mm.<sup>5</sup> Usually, 2–3 averages are acquired in each plane, adding to a total of ~11 minutes for T2W scans. Methods proposed to speed up T2W scan acquisition are classified into the acquisition of 3D T2WI as opposed to multiplanar 2D T2WI, acquisition of 2D TSE using radial acquisition, improvement of through-plane resolution, and adjusted acquisition parameters combined with AI-based reconstruction techniques (summarized in Table 2).

**ACQUISITION OF 3D T2W SCANS.** 3D imaging provides a continuous anatomical volume without slice gaps, with isotropic voxel size and limited geometric distortion. 3D imaging generally takes longer than 2D imaging, due to the acquisition of more lines. However, because of the isotropic resolution which can be achieved in 3D imaging, only one acquisition is needed making the overall scan time shorter than multiple 2D scans. Potential drawbacks include differences in image contrast and reduced in-plane resolution

compared to 2D acquisition. Hence, PI-RADS guidelines only recommend 3D imaging as an adjunct to 2D imaging.<sup>5</sup> In this section, shortening T2WI by using 3D instead of 2D imaging is treated.

Modifications can be applied to 3D imaging to maintain contrast similar to 2D imaging, and to accelerate acquisition while adhering to SAR limits as described by Mugler.<sup>10</sup> These modifications include the utilization of non-selective, short refocusing pulse trains, with reduced variable flip angles, which enable a long echo train, and in turn high resolution or low scan time. Such refinements to 3D T2WI are integrated into the following studies under discussion, which showcase comparable diagnostic performance in 2D and 3D T2WI. In a prospective study with 150 patients, a reduction of 40% in acquisition time was achieved.<sup>11</sup> In this study, two radiologists evaluating the image quality and diagnostic performance found no statistically significant difference between 3D and 2D imaging in terms of diagnostic accuracy. The single isotropic 3D T2W scan was found to be equivalent in terms of image quality, lesion delineation, characterization, and overall image quality compared to the longer multiplanar 2D T2W scans. Similarly, a retrospective study in 179 patients confirmed that 3D T2W scans are comparable to 2D T2W scans in terms of location, size, PI-RADS

TABLE 2. Summary of Methods for Speeding up T2W TSE

	Author	Number of Subjects; Type of Study	Method Used	Spatial Resolution (mm <sup>3</sup> )	FOV (mm <sup>2</sup> )	Averages	Total Acquisition Time (minutes:sec)
3D T2W TSE	Polancic et al. <sup>11</sup>	150 Pa; PS	C	0.6 × 0.6 × 3.0	200 × 200	3	11:14
	Choi et al. <sup>12</sup>	179 Pa; RS	P	0.8 × 0.8 × 0.8	320 × 320	2	3:35
			C	0.6 × 0.6 × 3.0 (ax), 0.3 × 0.3 × 3.0 (cor, sag)	180 × 180	2 (ax), 2 (cor), 6 (sag)	10:06
			P	0.3 × 0.3 × 0.6	200 × 200	2	4:55
	Bathala et al. <sup>13</sup>	69 Pa; RS	C	0.58 × 0.68 × 3.0	150 × 150	n/a	04:30 (ax)
Wong et al. <sup>14</sup>		26 Pa; RS	P	0.58 × 0.58 × 1.2	150 × 150	n/a	03:30 (ax)
			C	0.83 × 0.83 × 1.0	400 × 400	1	02:55 (1 avg)
			P	1.0 × 1.0 × 1.0	340 × 480	1-2	02:22 (1 avg), 04:44 (2 avg)
Shankar et al. <sup>16</sup>		11 Vo; PS	C	1.0 × 1.0 × 1.0	199 × 199	2	7:29
			P	1.0 × 1.0 × 1.0	299 × 299	1	2:45
Meier-Schroers et al. <sup>17</sup>		50 Pa; PS	C	1.15 × 1.15 × 3.0	420 × 420	n/a	07:53 (ax)
			P	1.15 × 1.15 × 3.0	420 × 420	n/a	05:29 (ax)
Bischoff et al. <sup>18</sup>		29 Pa; PS	C	0.35 × 0.35 × 3.0 (ax), 0.52 × 0.52 × 3.0 (sag)	180 × 180 (ax), 250 × 250 (sag)	n/a	03:51 (ax), 03:37 (sag)
			P	0.35 × 0.35 × 3.0 (ax), 0.52 × 0.52 × 3.0 (sag)	180 × 180 (ax), 250 × 250 (sag)	n/a	02:51 (ax), 02:02 (sag)
Improving through-plane resolution	Kargar et al. <sup>19</sup>	16 Pa; PS	C	0.75 × 0.75 × 3.0	240 × 240	4	04:14 (ax)
			P	1.0 × 1.0 × 1.0	72 × 204	2	6:38
Borisch et al. <sup>21</sup>		2 phantoms, 16 Pa; PS	C	0.62 × 0.71 × 3.0	200 × 200	2	n/a
			P	0.62 × 0.71 × 1.0	200 × n/a	2	6:20
Jurek et al. <sup>22</sup>	1 Pa; RS	C	0.63 × 0.63 × 3-4	200 × 200	n/a	11:29	
		P	0.63 × 0.63 × 0.63	200 × 200	n/a	4:05	

TABLE 2. Continued

Author	Number of Subjects; Type of Study	Method Used	Spatial Resolution (mm <sup>3</sup> )	FOV (mm <sup>2</sup> )	Averages	Total Acquisition Time (minutes:sec)
Gassenmaier et al. <sup>23</sup>	30 Pa; RS	C	0.3 × 0.3 × 3.0	200 × 200	3	04:37 (ax)
		P	0.3 × 0.3 × 3.0	200 × 200	1	01:38 (ax)
Gassenmaier et al. <sup>24</sup>	60 Pa; PS	C	0.3 × 0.3 × 3.0	200 × 200	3 (ax), 3 (cor), 2 (sag)	10:21
		P	0.3 × 0.3 × 3.0	200 × 200	1 (ax), 1 (cor), 1 (sag)	3:50
Park et al. <sup>25</sup>	109 Pa; RS	C	0.35 × 0.35 × 3.0	180 × 180	1.5	4:00
		P	0.35 × 0.35 × 3.0	180 × 180	1	2:30
Kim et al. <sup>26</sup>	46 Pa; RS	C	0.3 × 0.3 × 3.0	180 × 180	2	3:32
		P	0.4 × 0.4 × 3.0 (low res), 0.3 × 0.3 × 3.0 (high res)	180 × 180	1	00:52 (low res), 01:06 (high res)
Jung et al. <sup>27</sup>	40 Pa; RS and PS	C	0.28 × 0.28 × 3.0	180 × 180	2	3:16
		P	0.28 × 0.28 × 3.0	180 × 180	1-2	00:57-01:54
Liu et al. <sup>28</sup>	5 Pa; RS	C	0.6 × 0.6 × 0.6	n/a	n/a	n/a
		P	0.75 × 0.75 × 0.75	n/a	n/a	n/a
Harder et al. <sup>29</sup>	10 Vo and 23 Pa; PS	C	0.46 × 0.5 × 3.0	150 × 150	n/a	04:45 (ax)
		P	n/a	n/a	n/a	01:59; 02:36, 04:45 (ax)

Pa = patients; Vo = Volunteers; PS = prospective study; RS = retrospective study; C = conventional method; P = proposed method; Ax = axial; Sag = sagittal; Cor = coronal; Avg = average; n/a = not available.

classification, and evaluation of extra-prostatic extension of the largest, most aggressive lesion for each patient, based on the radiological evaluation performed by two radiologists.<sup>12</sup> In another retrospective comparison of 2D and 3D imaging on 69 patients,<sup>13</sup> three radiologists assessed the visibility of anatomic structures and overall image quality. No significant differences were found in the tissue contrast, overall image quality, and all anatomical structures assessed except for superior delineation of the genitourinary diaphragm in 3D imaging and seminal vesicles in 2D imaging. Quantitatively, the 2D images showed a slightly higher mean SNR in the peripheral zone. However, the authors concluded that 3D imaging is as robust in quality as conventional 2D imaging. Wong et al.<sup>14</sup> showed that 3D T2W scans could be acquired in an even shorter scan time by undersampling k-space, followed by compressed sensing (CS) based reconstruction, that is, an iterative reconstruction algorithm.<sup>15</sup> SNR, CNR, and delineation of the prostate were compared for regular and CS-reconstructed 3D T2W scans in a retrospective study of 26 patients. While the primary focus of this investigation was to accelerate radiotherapy planning, we have incorporated this technique into our review, emphasizing its potential to accelerate diagnostic scanning. Overall image quality and artifacts were evaluated by two MRI physicists, and ease of delineation was rated by two radiologists. Next to reducing acquisition time, all tested parameters were improved when CS was applied.

An alternative approach to performing 3D T2W acquisitions is by using a T2-prepared multishot 3D balanced steady-state free precession imaging sequence (T2prep-bSSFP) which takes only one-third of regular 2D acquisition time. The T2 preparation module is used to achieve rapid T2-weighting, while bSSFP acquisition results in high SNR per time. In a prospective investigation involving 11 volunteers, k-space was undersampled by a factor of 3 while the center 25% of k-space remained fully sampled.<sup>16</sup> A total variation regularized SENSE method was used for reconstruction. Two radiologists found T2prep-bSSFP images had reduced susceptibility to motion artifacts, comparable overall quality, contrast, and image sharpness, but lower subjective SNR compared to conventional T2WI.

In contrast to the consensus in PI-RADS, these studies suggest that 3D T2WI can replace 2D T2WI rather than just being an adjunct while reducing acquisition time despite unidentical soft tissue contrast. Only one study<sup>16</sup> reports a lower subjective SNR, which, however, does not limit the overall diagnostic quality.

**RADIAL ACQUISITION SCHEME.** Usually, T2W scans for prostate MRI are acquired with a Cartesian trajectory, sampling k-space along a regularly spaced cartesian grid. Another approach is using radial sampling by rotating each line around the center of k-space. Usually, in cartesian sampling, data is

oversampled to mitigate wrap-around artifacts, which increases the scan time. In radial sampling, the wrap-around artifact is replaced by streaking, and therefore oversampling of the k-space is not required, hence reducing the scan time. To further speed up radial acquisition, k-space can be sampled using multiple parallel phase-encoding lines called blades and combined with parallel imaging.

A prospective study in 50 patients compared the performance of a radial k-space acquisition scheme to a standard Cartesian 2D TSE.<sup>17</sup> While the main objective of this study was not to accelerate the acquisition, we find that the technique described still reduced the acquisition time. In this study, two radiologists found images acquired with the radial sequence superior with respect to motion robustness, image quality, detection rate, and lesion signal intensity. Although the radial acquisition resulted in a lower T2 contrast, there were no significant differences in PI-RADS scores when compared to conventional TSE. In another prospective study performed on 29 patients suspected of PCa, a conventional radial acquisition was compared to a CS-based reconstruction combined with radial acquisition. CS-based reconstruction of radial k-space enables higher subsampling rates, which translates to accelerated acquisition. This approach helps in the reconstruction of images from incoherently undersampled data such that the images are consistent with the actual measured data, while the noise-like artifacts are removed. By optimizing the regularization term, the level of data consistency, as well as the noise can be adjusted. Two radiologists found that in addition to a shorter scan time, CS-based reconstruction combined with radial acquisition resulted in decreased motion artifacts, improved image sharpness, enhanced overall image quality in both axial and sagittal planes. The use of CS with radial acquisition also resulted in significantly higher apparent SNR and CNR as compared to conventional radial acquisition, with these ratios based on signal intensity in the peripheral zone relative to the noise measured in muscle.<sup>18</sup> Furthermore, this technique improved lesion visibility in the sagittal plane and prostate capsule delineation in the axial plane.

In summary, the acquisition of T2W TSE imaging using radial trajectories leads to a faster acquisition but retains the image quality irrespective of lower contrast. CS reconstruction of undersampled data improves image quality, thus enabling further speeding up of acquisition.

**IMPROVING THROUGH-PLANE RESOLUTION.** An alternative approach to the acquisition of T2W TSE in three orthogonal planes is to perform acquisition solely in one orientation and enhance through-plane resolution in other orientations, resulting in a shorter scan time. A study conducted to test this approach used overlapping slices with small increments collected using a multislice acquisition in one orientation.<sup>19</sup> The reconstructed magnitude images were Fourier

transformed in the slice direction and subsequently filtered to improve through-plane resolution. The method was tested on a resolution phantom, prostate phantom, and prospectively acquired data from 16 patients. The through-plane resolution was improved to 1 mm by processing 3.2 mm thick slices. Three radiologists found that the proposed method leads to superior performance in terms of sharpness but inferior performance with respect to motion artifacts. To lower motion-related artifacts, this research group subsequently presented a data acquisition strategy in which each subset of simultaneously sampled slices was subdivided into multiple interleaved segments.<sup>20</sup> Incorporating this acquisition strategy, another study proposed a method for the reconstruction of 1 mm slices from overlapping 3 mm slices while retaining the SNR.<sup>21</sup> This study used wavelet sparsity-based regularization to reconstruct images with high through-plane resolution and improved SNR. This method was tested in vitro on contrast and resolution phantoms and in vivo in 16 patients. The wavelet sparsity regularization parameter was calibrated based on a radiological evaluation performed on six patients. According to two radiologists, relative SNR, contrast, fidelity of contrast, and sharpness of structures were all statistically superior in patient images. However, the clinical implementation of techniques<sup>21</sup> may be hindered due to their time intensive reconstruction processes that can take several hours to complete.

Yet another approach to improve the through-plane resolution is proposed by Jurek et al.<sup>22</sup> Although a slightly different method, that is, dictionary learning was used to achieve isotropic resolution computationally, similar to<sup>20,21</sup> a high-resolution image was acquired only in a single orientation (coronal), instead of acquiring images in three orientations which has a longer scan time. In this study, the dictionary was constructed from the acquired axial images of a single patient. The dictionary was subsequently used to reconstruct high-resolution axial slices from the acquired coronal images. A quantitative evaluation of the generated axial images was not possible due to the different in-plane voxel dimensions with the acquired axial slices. The generated images were found to be visually improved with respect to regular spline interpolation and similar to the acquired images, but the diagnostic quality remained unassessed.

Achieving a high through-plane resolution from a single acquisition can lead to a significant reduction in T2WI acquisition time. However, the generalizability and validity cannot be reliably asserted in the case of techniques tested on small samples (one patient)<sup>22</sup> and in studies lacking evaluation of the achieved diagnostic quality.

**AI-BASED RECONSTRUCTION APPROACHES.** T2WI acquisition parameters can be optimized such that the scan time is shortened. Such acquisitions should be followed by appropriate algorithms for the reconstruction of images with

sufficient diagnostic quality, which in recent years have heavily relied on deep learning (DL) techniques such as convolutional neural networks (CNNs) and generative adversarial networks (GANs). One approach is to sample fewer signal averages, followed by a complementary reconstruction method. In a retrospective investigation on 30 patients speeding up of mpMRI acquisition was demonstrated. In this study, only one average in the axial direction was acquired, followed by a CNN-based reconstruction.<sup>23</sup> In this study, two radiologists rated the CNN reconstructed images superior to the conventionally reconstructed images with three averages in terms of lesion detectability, diagnostic confidence, and overall image quality. In a prospective follow-up study, the network was used for the reconstruction of data in all three orientations.<sup>24</sup> The noise levels, artifacts, overall image quality, diagnostic confidence, and lesion conspicuity were evaluated to be superior in single average images reconstructed using a CNN as compared to conventional T2W TSE images by two radiologists. In a similar retrospective study carried out on 109 patients<sup>25</sup> the acquired averages were reduced from 1.5 to 1 in order to reduce the scan time. The images were subsequently reconstructed using a CNN. The SNR and CNR values were found to be significantly higher in CNN-reconstructed images compared to conventionally reconstructed images. However, overall image quality and lesion delineation quality were significantly reduced compared to conventionally acquired and reconstructed images, according to the three radiologists involved. The reduced image quality of CNN reconstructed images in this study contradicts the study of Gassenmaier et al.<sup>23,24</sup> but was attributed to the use of different acquisition parameters.

In addition to the acquisition of fewer averages, the scan time can be further shortened by doubling the parallel imaging (PI) factor. In a retrospective investigation of 46 patients, the quality of images acquired with fewer averages and double the PI factor was found to be similar to conventional T2WI in a shorter acquisition time<sup>26</sup> In this study, an unrolled variational network was used for the reconstruction of images. The conventional images were compared to two sets of images: one with a resolution equal to that of conventional TSE and another with a lower resolution. Two radiologists rated DL reconstructed T2WI superior to conventional T2WI, finding no differences in contrast ratios, sharpness of the anatomic structures, and qualitative factors such as lesion conspicuity and artifacts. The SNR and overall image quality for DL reconstructed-low resolution images were higher than DL reconstructed-conventional resolution images but not significantly higher than conventional T2WI. Another group acquired 2D TSE data with varying numbers of averages (2 for reference scan and 1–2 for accelerated scan) and parallel imaging factors (2 for reference scan, 4 for accelerated scan) and used a DL network for reconstruction.<sup>27</sup> This study was carried out on 155 patients. Two radiologists rated the

DL reconstructed images superior to conventional 2D TSE images. Accelerated DL reconstructed images showed lower normalized RMSE, higher SSIM, higher PSNR, and comparable lesion detection compared to conventional TSE. DL reconstructed images with two averages were found to be more clinically feasible than images with one average, with no parameter performing worse than conventional TSE.

A separate investigation involved the acquisition of low-resolution input data by adjusting the acquisition parameters and using GANs to synthesize diagnostic-quality images.<sup>28</sup> Images were acquired using a 2D low-resolution single-shot TSE (ss TSE) which takes only one-tenth of the total acquisition time of the conventional multiplanar T2W TSE. The proposed model generated isotropic volumes from both conventional and ssTSE scans of five patients, which were evaluated by a radiologist for imaging quality using the PI-RADS guidelines for delineation of capsule, seminal vesicles, neurovascular bundles, sphincter muscle and zonal distinction. Additionally, SSIM, PSNR, RMSE, and a perceptual score for GAN-generated images were assessed. Despite a slightly higher RMSE, GAN-generated high-resolution images outperformed in-plane ssTSE images in terms of perceptual quality and exhibited improved SSIM. The image quality was comparable to in-plane conventional images without sacrificing perceptual accuracy.

Finally, undersampling the k-space can also be implemented for faster acquisition. In case of an incoherently undersampled k-space, CS reconstruction can be used. Harder et al. combined CS with an iterative learning-based reconstruction scheme that enhances the conventional CS approach.<sup>29</sup> Conventionally in CS, a wavelet transform is used, but in this work, an iterative network acts as the sparsifying transform in the CS algorithm. The parallel imaging approach ensures data consistency and incorporates coil sensitivity distribution and location of the image background. In this study, T2WI data was acquired by undersampling the k-space in a pseudorandom, density-weighted pattern with higher sampling density towards the k-space center. The study was carried out prospectively on ten volunteers and 23 patients with three acceleration factors (4.8, 3.4, and 1.7). Image analysis was performed independently by radiologists comparing images reconstructed using the adaptive algorithm to images reconstructed using conventional CS (acceleration factor = 1.7). The iterative learning-based-CS-reconstructed images demonstrated higher CNR and SNR, better lesion detection and image quality, higher diagnostic certainty, sharper images, fewer artifacts, and lesser noise compared to reference standard CS images.

### Speeding up Diffusion-Weighted Imaging

DWI is used for signal contrast generation based on the difference in Brownian motion of water molecules between tissue and tumors. ADC maps are used to quantify diffusion and are used for treatment response evaluation and

assessment of tumor progression. Typically, in the mpMRI protocol, DWI scans take about 3.5 minutes. In most clinical implementations, DWI consists of at least two diffusion weightings, so-called  $b$ -values, and a monoexponential model of signal decay to calculate ADC values.<sup>5</sup> We review techniques for speeding up DWI by synthesis of higher  $b$ -value DWI, synthesis of ADC, using a reduced field of view (FOV), or using a modified pulse sequence (summarized in Table 3). Similar to T2WI, there is a growing role of deep learning-based models in reconstruction.

**SYNTHESIZED HIGH B-VALUE DWI.** Multiple  $b$ -values are generally acquired and used for the calculation of the ADC using a monoexponential model of signal decay. Ambiguity exists over the optimal  $b$ -values, diffusion weighting, and the number of  $b$ -values that should be acquired. In comparison to ADC maps alone, sometimes tumor conspicuity is improved in high  $b$ -value images. However, higher  $b$ -values require longer acquisition times and may result in poor image quality due to low SNR and geometric distortion. To address these challenges, some studies propose to generate high  $b$ -value images from acquired lower  $b$ -values.

A retrospective study performed on 124 patients compared the performance of generated high  $b$ -value images ( $b$ -2000 and  $b$ -2500) extrapolated from lower  $b$ -values with acquired high  $b$ -value images ( $b$ -2000).<sup>30</sup> According to four radiologists, both extrapolated  $b$ -values separately showed significantly better background signal suppression, better anatomic clarity, greater lesion conspicuity, comparable tumor detection rate, and less distortion compared to the acquired high  $b$ -value DWI. One notable downside was worsened ghosting. Another study recommends the synthesis of high  $b$ -value DWI ( $b$ -1500) using a GAN.<sup>31</sup> In this retrospective investigation of 299 patients, six radiologists evaluated the image quality. The GAN-synthesized high  $b$ -value DWI showed clear contours of the prostate and lesions, high suppression of normal and benign prostate tissue, and fewer artifacts and noise compared to the acquired data. The amount of distortion was similar between the two types of images. Alternatively, complex-valued averaging of images without explicitly performing a phase correction of the single images can be performed to improve the image quality of calculated high  $b$ -value DWIs. This approach should lead to enhanced SNR and eliminate haze-like backgrounds which are typically observed in low signal regions when magnitude averaging is implemented. In a retrospective study conducted on 84 patients, two radiologists evaluating the images found complex-averaged calculated high  $b$ -values yielded higher diagnostic accuracy for detecting significant prostate lesions compared to magnitude-averaged acquired high  $b$ -values.<sup>32</sup> The complex-averaged images showed no noise bias in low signal regions, resulting in sharper images and potentially enhanced diagnostic accuracy. Additionally, it was found that



TABLE 3. Summary of Methods for Speeding up DWI

	Author	Number of Subjects; Type of Study	Method Used	Spatial Resolution (mm <sup>3</sup> )	FOV (mm <sup>2</sup> )	b-values (Averages)	Total Acquisition Time (minutes:sec)
Synthesizing High b-value DWI	Jendoubi et al. <sup>30</sup>	124 Pa; RS	C	2 × 2 × 4	200 × 50	2000 (16)	04:20 (ax)
			P	2 × 2 × 4	200 × 50	100 (2), 400 (5), 800 (10)	03:54 (ax)
	Hu et al. <sup>31</sup>	299 Pa; RS	C	2.13–4.68 × 1.58–2.29 × 3–4	300–380 × 210–380	0–50 (n/a), 800–1000 (n/a), 1500 (n/a)	3:05–4:43
			P	1.96 × 1.09 × 3	300–380 × 210–380	0–50 (n/a), 800–1000 (n/a)	n/a
Synthesizing ADC	Kordhbacheh et al. <sup>32</sup>	84 Pa; RS	C	1.92 × 1.92 × 3	220 × 220	2000 (15)	5:20
			P	1.92 × 1.92 × 3	220 × 220	50 (2), 900 (9)	2:55
	Xi et al. <sup>33</sup>	43 Pa; RS	C	1.25 × 1.30 × 3	160 × 180	0 (1), 10 (1), 25 (1), 50 (1), 100 (1), 250 (1), 450 (1), 1000 (2), 1500 (3), 2000 (5)	6:30
Reduced FOV	Hu et al. <sup>34</sup>	50 Pa and 10 Vo; PS	C	2.13 × 2.13 × 3.3	380 × 280	50 (n/a), 1000 (n/a), 1500 (n/a)	*
			P	0.95 × 0.95 × 3.3	190 × 106	1000 (n/a)	*
	Kaye et al. <sup>35</sup>	37 Pa; RS	C	1.25–2.4 × 2.5–3 × 4	200–240 × 200–240	0, 50 (2–4), 1000 (16)	2:40
			P	1.80–2.16 × 0.84–1.01 × 4	200–240 × 200–240	0, 50 (2–4), 1000 (2)	0:48
Warddahl et al. <sup>36</sup>		43 Pa; RS	C	1.2 × 1.25 × 3	240 × 240	0 (8), 100 (6), 1000 (12)	5:30
			P	1.5 × 1.5 × 4–5	240 × 120	100 (6), 1000 (16)	4:30
	Lee et al. <sup>37</sup>	50 Pa; RS	C	1.8 × 2.2 × 4	200 × 220	50 (2), 400 (3), 1000 (10), 1400 (10)	5:24
		P	1.1 × 2 × 4	112 × 200	50 (2), 1400 (10)	3:12	

TABLE 3. Continued

Author	Number of Subjects; Type of Study	Method Used	Spatial Resolution (mm <sup>3</sup> )	FOV (mm <sup>2</sup> )	b-values (Averages)	Total Acquisition Time (minutes:sec)
Ma et al. <sup>38</sup>	32 Pa; RS	C	1.4 × 1.4 × 4	260 × 260	0 (n/a), 2000 (n/a)	10:11
		P	1.4 × 1.4 × 4	160 × 72	0 (n/a), 2000 (n/a)	9:02
Zhang et al. <sup>39</sup>	10 Vo, 5 Pa, phantom, ex-vivo prostate specimen; PS	C	1.0–1.6 × 1.0–1.6 × 3.6	260 × 216	0 (7), 100 (7), 400 (7), 800 (7)	5:53
		P	1.0–1.6 × 1.0–1.6 × 3.6	260 × 216	0 (5), 100 (5), 400 (5), 800 (5)	4:12
Zhang et al. <sup>40</sup>	27 Pa; PS	C	2 × 2 × 4.8	120 × 240	100 (6), 800 (12)–1500 (15)	04:00–07:00
		P	2 × 2 × 4.8	120 × 240	100 (6), 800 (15)	4:16
Hosseiny et al. <sup>41</sup>	162 Pa; PS	C	1.6 × 1.6 × NA	260 × 153	0 (7), 100 (7), 400 (7), 800 (7)	6:02
		P	2.0 × 2.0 × NA	220 × 220	50 (1), 800 (2)	4:47
Liu et al. <sup>42</sup>	53 Pa; RS	C	0.75 × 0.85 × 4 (T2WI) 1.41 × 1.41 × 4 (DWI)	240 × 240 (T2WI) 260 × 260 (DWI)	n/a (T2WI), 1000 (n/a) (DWI)	6:10
		P	0.50 × 0.89 × 1 (T2WI) 1.41 × 1.41 × 4 (DWI)	120 X 180 (T2WI) 260 × 260 (DWI)	n/a (T2WI), 1000 (n/a) (DWI)	4:30
Weiss et al. <sup>43</sup>	52 Pa; PS	C	2 × 2 × 3	110 × 100	0 (4), 1500 (10)	4:20
		P	2 × 2 × 3	110 × 100	0 (4), 1500 (10)	1:53

Pa = patients; Vo = volunteers; PS = prospective study; RS = retrospective study; C = conventional method; P = proposed method; Ax = axial; n/a = not available; \* = acquisition time indiscernible from given data.

acquired and calculated high  $b$ -value DWI ( $b$ -2000) performed similarly in terms of accuracy, image quality, and detection of clinically significant PCa.

**SYNTHESIZED ADC.** ADC maps can be calculated from DWI and are integral to the detection and staging of PCa. Lower ADC values are observed in cancerous tissues compared to benign prostate tissue helping cancer detection. Reducing the number of  $b$ -values required to calculate the ADC results in a reduced acquisition time. However, ADCs rely on the quality of the DWI input.

A study comparing synthetic ADC maps generated using only two  $b$ -values to conventional ADC maps created using a monoexponential fitting using multiple  $b$ -values was conducted retrospectively on 43 patients.<sup>33</sup> The synthetic ADC is a normalized ratio of signal intensities observed in two  $b$ -values images. Xi et al. determined an optimal high-low  $b$ -values combination (low  $b$ -100 with high  $b$ -1500 or  $b$ -2000) yielding the highest CNR for the prostate. According to two radiologists, the difference between normal and cancerous tissues observed using synthetic ADC maps was non-inferior to that of conventional maps, quantitatively and qualitatively. In another prospective study, ADCs with a reduced FOV and increased resolution were synthesized using only one full FOV  $b$ -value ( $b$ -50,  $b$ -1000, or  $b$ -1500) using a GAN.<sup>34</sup> Two radiologists evaluated the synthesized ADC maps for 50 patients and 10 volunteers. Compared to conventional ADCs, synthesized ADCs demonstrated better image quality, higher accuracy, and reproducibility. While noise distribution, image structure, and features were comparable, tumor detection and classification performance were superior in the ADC synthesized from a  $b$ -1000 acquisition.

A different technique to accelerate the scanning process is utilizing a reduced number of averages for acquisition of  $b$ -values, which will subsequently be used for synthesizing ADC maps. This technique was implemented in a retrospective study undertaken on 37 patients. The associated drawbacks were mitigated by denoising the DWI scans through novel DL-based reconstruction techniques.<sup>35</sup> In this study, qualitative evaluation of the denoised high  $b$ -values DWI scans was performed by two radiologists. The CNN-denoised images were found to have a significantly greater probability of scoring higher in terms of image quality, noise suppression, image sharpness, and lesion conspicuity compared with conventional high  $b$ -value DWI. The ADC maps based on the denoised images appeared similar to conventional high  $b$ -value DWI while requiring a shorter scan time.

**REDUCED FOV.** A reduced FOV acquisition using 2D selective RF pulse enables faster acquisition by decreasing the number of phase-encoding lines acquired. This approach also helps minimize distortions caused by field inhomogeneity or susceptibility artifacts due to factors like rectal air or metal

from prosthetics. A retrospective study conducted on 43 patients compared a reduced FOV sequence utilizing a 90° 2D-spatially selective pulse to a conventional DWI sequence.<sup>36</sup> Two radiologists evaluated the images with respect to overall distortion and image quality based on PI-RADS guidelines. The distortion was less in reduced FOV images leading to better image quality, while the mean ADC values were similar in reduced FOV and conventional DWI.

A modified reduced FOV DWI sequence was presented in another study, wherein the slice selection gradient of a 2D-selective RF pulse was tilted to allow rotation of the side excitations, leading to reduced aliasing artifacts, reduced echo time, and increased SNR.<sup>37</sup> In this retrospective study conducted on 50 patients, two radiologists found that the modified reduced FOV DWI showed better overall image quality, discernibility of anatomic regions, and lesion conspicuity with fewer artifacts, and comparable ADC contrast, compared to a regular reduced FOV DWI. Mean ADC values of tumors and surrounding tissue peripheral zones were similar in modified and regular reduced FOV DWI, but significantly higher compared to conventional DWI. In a similar study, a retrospective comparison of 32 patients was conducted, examining the use of reduced FOV high  $b$ -value DWI based on a 2D-selective excitation pulse in comparison to conventional high  $b$ -value DWI scans.<sup>38</sup> 2D pulses have the ability to mitigate single-shot echo-planar imaging (ss EPI) related artifacts and distortions, which affect image quality and diagnostic performance at high  $b$ -values. Four radiologists rated the reduced FOV DWI sequence significantly better in terms of explicit visibility of anatomical structures within the prostate, demarcation of the prostate gland, susceptibility artifacts, distortion, and overall image quality. The reduced FOV DWI led to better image quality and diagnostic performance, with a higher tumor detection rate and more precise staging for PCa while also reducing total acquisition time.

**ADJUSTED PULSE SEQUENCE.** Modifications in the acquisition parameters can help suppress artifacts related to eddy currents, susceptibility, distortion, etc., and to improve SNR, thus improving the overall image quality compared to conventional acquisitions. Occasionally, using such acquisition schemes can help shorten the acquisition time while the imaging quality is retained.

One such approach is employing an optimized encoding scheme to ensure the preservation of SNR, even when a reduced number of averages is acquired. Zhang et al. hypothesize that fewer averages can be acquired for DWI while maintaining sufficient SNR, by adjusting magnetic gradients for an optimized diffusion encoding scheme that is capable of suppressing eddy current-induced distortion artifacts and facilitating improvement in SNR for a given  $b$ -value and EPI readout duration.<sup>39</sup> In this study, carried out prospectively on 10 volunteers, 5 patients, a phantom, and an ex-vivo prostate specimen to compare the optimized diffusion encoding to

conventional unipolar and bipolar encoding schemes, three radiologists found that the optimized encoding scheme demonstrated  $\geq 25\%$  higher SNR and had similar or higher image quality compared to bipolar encoding while also reducing eddy current effects. A different approach was employed in a prospective study of 27 patients. Stimulated-echo (STE) DWI at a single moderate  $b$ -value ( $b=800/1000$ ) has the potential to mitigate drawbacks associated with the acquisition of high  $b$ -values, while providing high CNR and reliable ADC mapping due to shorter TE.<sup>40</sup> Three radiologists found that an STE DWI acquisition with a moderate  $b$ -value had superior SNR and comparable CNR and lesion detectability compared to conventional high  $b$ -value images. For overall image quality and diagnostic confidence, a single STE moderate  $b$ -value was found to be comparable to the conventional high  $b$ -values and surpassed conventional moderate  $b$ -values according to two out of three readers, indicating that a single moderate STE DWI may provide sufficient image quality and quantitative reliability within a shorter scan time, in place of two DWI acquisitions (with moderate and high  $b$ -value).

To decrease susceptibility sensitivity, reduce image distortion and improve image quality for lesion detection and delineation compared to conventional ss EPI acquisition, a readout segmented echoplanar imaging (rs EPI) is recommended as an alternative.<sup>41</sup> In a prospective study conducted on 162 patients, two radiologists evaluated the images and rated rs EPI significantly higher in image quality, better in lesion conspicuity and anatomic delineation, and more resistant to geometrical distortion. With shorter acquisition time due to larger voxel size, fewer  $b$ -values, and less averages, rs EPI showed significantly improved lesion conspicuity and could be used as an alternative or replacement for acquiring prostate DWI instead of ss EPI.

Finally, the simultaneous acquisition of T2WI and DWI can be leveraged to speed up scanning. A retrospective study on 53 patients evaluated simultaneous acquisition through scan interleaving of 3D T2WI and 2D DWI during one repetition time.<sup>42</sup> In this study, each shot of the DWI scan was interleaved between two repeated cycles of a 3D T2WI. The quality of images was evaluated by two radiologists with regard to sharpness, contrast, deformation, and image artifact. Simultaneous acquisitions demonstrated better lesion delineation and higher contrast ratio, with diagnostic accuracy similar to conventional acquisitions, while requiring less acquisition time. Another short scanning protocol wherein the DWI sequence was acquired using simultaneous multislice (SMS) acquisition, which excites and acquires multiple slices simultaneously, thus shortening the scan time, was tested prospectively on 52 patients.<sup>43</sup> In this study, in addition to the SMS DWI acquisition, T2WI was performed in only one orientation. Two radiologists found the diagnostic performance similar to the conventional protocol in terms of PI-RADS score, anatomical localization, lesion detection, and

ADC calculation. Moreover, in three patients, suspicious lymph nodes were reported as additional findings which were found to be equally detectable in both protocols. However, additional sequences may be required for specific clinical queries, such as capsular involvement and location of tumor with respect to other pelvic organs, or for detection of small significant tumors.

## Discussion

In this review, we explore methods proposed to reduce the acquisition time of the mpMRI protocol by adjusting the T2-weighted and diffusion-weighted imaging. Due to constant updates in the field, we focus on studies published after 2017. We present a concise technical overview of these speeding-up methods, which can serve as a foundation for future implementations of faster mpMRI protocols.

Accelerating the mpMRI protocol while preserving diagnostic quality may be achieved through various approaches, such as acquiring undersampled data or adjusting acquisition parameters, or the pulse sequence followed by complementary reconstruction techniques such as those based on AI or CS. Moreover, acquiring fewer  $b$ -values, and employing AI-based synthesis of high  $b$ -value images or ADC may facilitate faster DWI scans. Combining multiple techniques could lead to even faster scans.

Contrary to the PI-RADS guidelines, we find evidence that the 3D T2WI may be an effective alternative to 2D T2WI, providing comparable diagnostic quality rather than being used solely as a supplementary tool.<sup>11–14,16</sup> Furthermore, in context of 2D T2WI, a valid apprehension is that the utilization of DL or CS-based reconstruction techniques for undersampled data may introduce image blurring, which could in turn contribute to unclear borders of TZ lesions leading to a higher PI-RADS score and increasing the likelihood of false positives. However, the studies of Gassenmaier et al.<sup>23,24</sup> did not show this effect and even showed a higher diagnostic accuracy for both TZ and PZ lesions using DL-based reconstruction. Additionally, the radial acquisition of T2W TSE leading to a faster acquisition, while retaining the image quality irrespective of lower contrast may also hold potential for further development of faster acquisition of mpMRI.<sup>17,18</sup> It is important to highlight that while scanning fewer planes accelerates the scanning, it may compromise the diagnostic accuracy as the unscanned third plane may aid in defining the extent of the lesion beyond the prostate capsule. As demonstrated by Kargar et al., Borisch et al., and Jurek et al.,<sup>19,21,22</sup> methods like filtering, wavelet sparsity-based regularization or dictionary learning have been recommended to enhance the resolution of the unscanned planes. For DWI, AI-based applications for synthesizing high  $b$ -value DWI or generating ADC maps demonstrate comparable performance

to conventional methods of high  $b$ -value acquisition and ADC generation.<sup>31–35</sup>

To ensure successful implementation in clinical practice, the proposed methods must exhibit diagnostic quality comparable to conventional techniques. Radiological evaluation plays a critical role in this assessment, as quantitative metrics may not fully reflect diagnostic quality. Therefore, diagnostic evaluation by radiologists or diagnostic AI in prospectively conducted studies is crucial for validating these methods and adhering to PI-RADS guidelines. All studies highlighted in this review rely on radiological evaluation for validation of diagnostic quality, except for Jurek et al.<sup>22</sup> Additionally, while some studies highlighted in this review have relatively small sample sizes<sup>22</sup> careful consideration of data variability, required diagnostic quality, and practical constraints is necessary when determining sample sizes for the validation of new techniques. Moreover, for studies suggesting undersampling for faster acquisition, prospectively acquired data provides stronger evidence of the effectiveness and overall diagnostic performance and the actual shortening of acquisition time, than retrospectively undersampled data which might not take physical sampling constraints into account. Diagnostic evaluation and agreement are essential for accepting techniques that offer faster scans with sensitivity and specificity similar to the mpMRI protocol, even if they may have slightly lower image quality.

Beyond accelerating T2WI and DWI, optimizing the planning of the scan and positioning of the patient within the scanner, possibly with the help of AI as demonstrated by Brown and Marotta, Edalati et al., and Muelly et al.<sup>44–46</sup> will also contribute to better management of the increasing number of PCa patients. Furthermore, improvements in scanner hardware such as using stronger gradients or improved receive coils might also contribute toward achieving superior SNR, which in turn can be exchanged for decreased scan time. Tenbergen et al.<sup>47</sup> summarized various coil designs facilitating prostate imaging in high fields in their review. Moreover, the feasibility of accelerating prostate imaging at high field strength, provided appropriate coil technology is used to adhere to specific absorption rate limits has been shown by Maas et al.<sup>48</sup> However, in this review, our sole focus is on advancements based on altering imaging sequences and reconstruction, therefore improvements related to hardware modifications are not discussed.

The selection criteria employed in this review introduce certain limitations in terms of the studies included. In our review, we do not highlight speeding up by using the bpMRI protocol as they are discussed in detail in the reviews of Hotker et al.<sup>7</sup> and Girometti et al.<sup>8</sup> Additionally, based on our inclusion criteria, we observed that not all articles meeting the criteria adhered to the PI-RADS guidelines with respect to spatial resolution. However, all methods aimed at accelerating acquisition should perform equally well on higher-resolution sequences.

## Conclusions

In summary, there is a noticeable trend towards adopting techniques involving undersampled data, reducing the number of averages, or utilizing fewer lower  $b$ -values. Incorporating AI or other reconstruction methods like CS can mitigate drawbacks associated with unconventional acquisition approaches. If diagnostic quality remains high despite a slight deterioration in image quality, acceleration factors can be enhanced further. Successful implementation and validation of these methods depend on radiological evaluation and adherence to PI-RADS guidelines.

## Funding Information

This research was financially supported by the PPP Allowance made available by Health~Holland, Top Sector Life Sciences & Health, to stimulate public-private partnerships and by Siemens Healthineers.

## Declaration of Research Support

Jurgen Fütterer declares to receive research support from Siemens Healthineers, the other authors declare that they have no competing interests.

## References

1. Sung H, Ferlay J, Siegel R, et al. Global cancer statistics 2020: GLOBOCAN estimates of incidence and mortality worldwide for 36 cancers in 185 countries. *CA Cancer J Clin* 2021;71(3):209-249.
2. Ferlay J, Colombet M, Soerjomataram I, et al. *Global cancer observatory: Cancer tomorrow*. Lyon, France: International Agency for Research on Cancer; 2020. Available from: <https://gco.iarc.fr/tomorrow>, accessed [20 April 2023].
3. Wysock JS, Lepor H. Multi-parametric MRI imaging of the prostate-implications for focal therapy. *Transl Androl Urol* 2017;6(3):453-463.
4. Fam MM, Yabes JG, Macleod LC, et al. Increasing utilization of multiparametric magnetic resonance imaging in prostate cancer active surveillance. *Urology* 2019;130:99-105.
5. Turkbey B, Rosenkrantz AB, Haider MA, et al. Prostate imaging reporting and data system version 2.1: 2019 update of prostate imaging reporting and data system version 2. *Eur Urol* 2019;76(3):340-351. <https://doi.org/10.1016/j.eururo.2019.02.033>.
6. Barentsz JO, Richenberg J, Clements R, et al. ESUR prostate MR guidelines 2012. *Eur Radiol* 2012;22(4):746-757.
7. Hotker AM, Vargas HA, Donati OF. Abbreviated MR protocols in prostate MRI. *Life (Basel)* 2022;12(4):552.
8. Girometti R, Cereser L, Bonato F, Zuiani C. Evolution of prostate MRI: From multiparametric standard to less-is-better and different-is better strategies. *Eur Radiol Exp* 2019;3(1):5.
9. Page MJ, McKenzie JE, Bossuyt PM, et al. The PRISMA 2020 statement: An updated guideline for reporting systematic reviews. *Syst Rev* 2021;10(1):89.
10. Mugler JP 3rd. Optimized three-dimensional fast-spin-echo MRI. *J Magn Reson Imaging* 2014;39(4):745-767.
11. Polanec SH, Lazar M, Wengert GJ, et al. 3D T2-weighted imaging to shorten multiparametric prostate MRI protocols. *Eur Radiol* 2018;28(4):1634-1641.
12. Choi MH, Lee YJ, Jung SE, Han D. High-resolution 3D T2-weighted SPACE sequence with compressed sensing for the prostate gland:

- Diagnostic performance in comparison with conventional T2-weighted images. *Abdom Radiol (NY)*. 2023;48(3):1090-1099.
13. Bathala TK, Venkatesan AM, Ma JF, et al. Quality comparison between three-dimensional T2-weighted SPACE and two-dimensional T2-weighted turbo spin echo magnetic resonance images for the brachytherapy planning evaluation of prostate and periprostatic anatomy. *Brachytherapy* 2020;19(4):484-490.
  14. Wong OL, Poon DMC, Kam MKM, et al. 3D-T2W-TSE radiotherapy treatment planning MRI using compressed sensing acceleration for prostate cancer: Image quality and delineation value. *Asia Pac J Clin Oncol* 2022;18(5):E369-E377.
  15. Lustig M, Donoho D, Pauly JM. Sparse MRI: The application of compressed sensing for rapid MR imaging. *Magn Reson Med* 2007;58(6):1182-1195.
  16. Shankar RV, Rocca E, Cruz G, et al. Accelerated 3D T2w-imaging of the prostate with 1-millimeter isotropic resolution in less than 3 minutes. *Magn Reson Med* 2019;82(2):721-731.
  17. Meier-Schroers M, Marx C, Schmeel FC, et al. Revised PROPELLER for T2-weighted imaging of the prostate at 3 tesla: Impact on lesion detection and PI-RADS classification. *Eur Radiol* 2018;28(1):24-30.
  18. Bischoff LM, Katemann C, Isaak A, et al. T2 turbo spin Echo with compressed sensing and Propeller acquisition (sampling k-space by utilizing rotating blades) for fast and motion robust prostate MRI: Comparison with conventional acquisition. *Invest Radiol* 2023;58(3):209-215.
  19. Kargar S, Borisch EA, Froemming AT, et al. Use of kZ-space for high through-plane resolution in multislice MRI: Application to prostate. *Magn Reson Med* 2019;81(6):3691-3704.
  20. Kargar S, Borisch EA, Froemming AT, et al. Modified acquisition strategy for reduced motion artifact in super resolution T2 FSE multislice MRI: Application to prostate. *Magn Reson Med* 2020 Nov;84(5):2537-2550.
  21. Borisch EA, Froemming AT, Grimm RC, Kawashima A, Trzasko JD, Riederer SJ. Model-based image reconstruction with wavelet sparsity regularization for through-plane resolution restoration in T-2-weighted spin-echo prostate MRI. *Magn Reson Med* 2023;89(1):454-468.
  22. Jurek J, Kocinski M, Materka A, et al. Dictionary-based through-plane interpolation of prostate cancer T2-weighted MR images. 22<sup>nd</sup> SPA 2018: Signal Processing: Algorithms Architectures Arrangements and Applications: Conference Proceedings, IEEE Poland Section Circuits and Systems Chapter, September 19th-21st 2018, Poznan Poland; IEEE. Piscataway, New Jersey; pp. 168-173.
  23. Gassenmaier S, Afat S, Nickel D, Mostapha M, Herrmann J, Othman AE. Deep learning-accelerated T2-weighted imaging of the prostate: Reduction of acquisition time and improvement of image quality. *Eur J Radiol* 2021;137:109600.
  24. Gassenmaier S, Afat S, Nickel MD, et al. Accelerated T2-weighted TSE imaging of the prostate using deep learning image reconstruction: A prospective comparison with standard T2-weighted TSE imaging. *Cancers (Basel)*. 2021;13(14):3593.
  25. Park JC, Park KJ, Park MY, Kim MH, Kim JK. Fast T2-weighted imaging with deep learning-based reconstruction: Evaluation of image quality and diagnostic performance in patients undergoing radical prostatectomy. *J Magn Reson Imaging* 2022;55(6):1735-1744.
  26. Kim EH, Choi MH, Lee YJ, Han D, Mostapha M, Nickel D. Deep learning-accelerated T2-weighted imaging of the prostate: Impact of further acceleration with lower spatial resolution on image quality. *Eur J Radiol* 2021;145:110012.
  27. Jung W, Kim EH, Ko J, Jeong G, Choi MH. Convolutional neural network-based reconstruction for acceleration of prostate T-2 weighted MR imaging: A retro- and prospective study. *Br J Radiol* 2022;95(1133):20211378.
  28. Liu YC, Liu YL, Vanguri R, et al. 3D isotropic super-resolution prostate MRI using generative adversarial networks and unpaired multiplane slices. *J Digit Imaging* 2021;34(5):1199-1208.
  29. Harder FN, Weiss K, Amiel T, et al. Prospectively accelerated T2-weighted imaging of the prostate by combining compressed SENSE and deep learning in patients with histologically proven prostate cancer. *Cancers (Basel)* 2022;14(23):5741.
  30. Jendoubi S, Wagner M, Montagne S, et al. MRI for prostate cancer: Can computed high b-value DWI replace native acquisitions? *Eur Radiol* 2019;29(10):5197-5204.
  31. Hu L, Zhou DW, Zha YF, et al. Synthesizing high-b-value diffusion-weighted imaging of the prostate using generative adversarial networks. *Radiol Artif Intell* 2021;3(5):e200237.
  32. Kordbacheh H, Seethamraju RT, Weiland E, et al. Image quality and diagnostic accuracy of complex-averaged high b value images in diffusion-weighted MRI of prostate cancer. *Abdom Radiol (NY)* 2019;44(6):2244-2253.
  33. Xi Y, Liu A, Olumba F, et al. Low-to-high b value DWI ratio approaches in multiparametric MRI of the prostate: Feasibility, optimal combination of b values, and comparison with ADC maps for the visual presentation of prostate cancer. *Quant Imaging Med Surg* 2018;8(6):557-567.
  34. Hu L, Zhou DW, Fu CX, et al. Calculation of apparent diffusion coefficients in prostate cancer using deep learning algorithms: A pilot study. *Front Oncol* 2021;11:697721.
  35. Kaye EA, Aherne EA, Duzgol C, et al. Accelerating prostate diffusion-weighted MRI using a guided denoising convolutional neural network: Retrospective feasibility study. *Radiol Artif Intell*. 2020;2(5):e200007.
  36. Warndahl BA, Borisch EA, Kawashima A, Riederer SJ, Froemming AT. Conventional vs. reduced field of view diffusion weighted imaging of the prostate: Comparison of image quality, correlation with histology, and inter-reader agreement. *Magn Reson Imaging* 2018;47:67-76.
  37. Lee EJ, Hwang J, Chang YW, et al. Modified reduced field-of-view diffusion-weighted magnetic resonance imaging of the prostate: Comparison with reduced field-of-view imaging and single shot Echo-planar imaging. *J Comput Assist Tomogr* 2021;45(3):367-373.
  38. Ma S, Xu K, Xie H, et al. Diagnostic efficacy of b value (2000 s/mm<sup>2</sup>) diffusion-weighted imaging for prostate cancer: Comparison of a reduced field of view sequence and a conventional technique. *Eur J Radiol* 2018;107:125-133.
  39. Zhang ZH, Moulin K, Aliotta E, et al. Prostate diffusion MRI with minimal echo time using eddy current nulled convex optimized diffusion encoding. *J Magn Reson Imaging* 2020;51(5):1526-1539.
  40. Zhang Y, Wells SA, Triche BL, Kelcz F, Hernando D. Stimulated-echo diffusion-weighted imaging with moderate b values for the detection of prostate cancer. *Eur Radiol* 2020;30(6):3236-3244.
  41. Hosseiny M, Sung KH, Felker E, et al. Read-out segmented Echo planar imaging with two-dimensional navigator correction (RESOLVE): An alternative sequence to improve image quality on diffusion-weighted imaging of prostate. *Br J Radiol* 2022;95(1136):20211165.
  42. Liu Y, Wang W, Qin XB, et al. The applied research of simultaneous image acquisition of T2-weighted imaging (T2WI) and diffusion-weighted imaging (DWI) in the assessment of patients with prostate cancer. *Asian J Androl* 2019;21(2):177-182.
  43. Weiss J, Martirosian P, Notohamiprodjo M, et al. Implementation of a 5-minute magnetic resonance imaging screening protocol for prostate cancer in men with elevated prostate-specific antigen before biopsy. *Invest Radiol* 2018;53(3):186-190.
  44. Brown AD, Marotta TR. Using machine learning for sequence-level automated MRI protocol selection in neuroradiology. *J Am Med Inform Assoc* 2018;25(5):568-571.
  45. Edalati M, Zheng Y, Watkins MP, et al. Implementation and prospective clinical validation of AI-based planning and shimming techniques in cardiac MRI. *Med Phys* 2022;49(1):129-143.
  46. Muellly M, Stoddard P, Vasana S. Using machine learning with dynamic exam block lengths to decrease patient wait time and optimize MRI schedule fill rate. In: Proceedings of the 26th Annual Meeting of ISMRM, Honolulu, 2017.
  47. Tenbergen CJA, Metzger GJ, Scheenen TWJ. Ultra-high-field MR in prostate cancer: Feasibility and potential. *Magma* 2022;35(4):631-644.
  48. Maas MC, Vos EK, Lagemaat MW, et al. Feasibility of T2-weighted turbo spin echo imaging of the human prostate at 7 tesla. *Magn Reson Med* 2014;71(5):1711-1719.